Electronic Supplementary Material (ESI) for Journal of Materials Chemistry C.

Supporting Information

Highly fluorescent nitrogen-doped carbon dots with large Stokes shifts

Xueqiao Zhang, [a†] Ye Liu,[a†] Chieh-Hsi Kuan,[b] Longteng Tang, [b] Taylor D. Krueger,[b] Sanjida Yeasmin, [a] Ahasan Ullah, [a] Chong Fang,[b] and Li-Jing Cheng*[a]

[a]School of Electrical Engineering and Computer Science, Oregon State University, Corvallis, Oregon 97331, USA

[b]Department of Chemistry, Oregon State University, Corvallis, Oregon 97331, USA

†These authors contributed equally.

*Corresponding Author, Email: chengli@oregonstate.edu

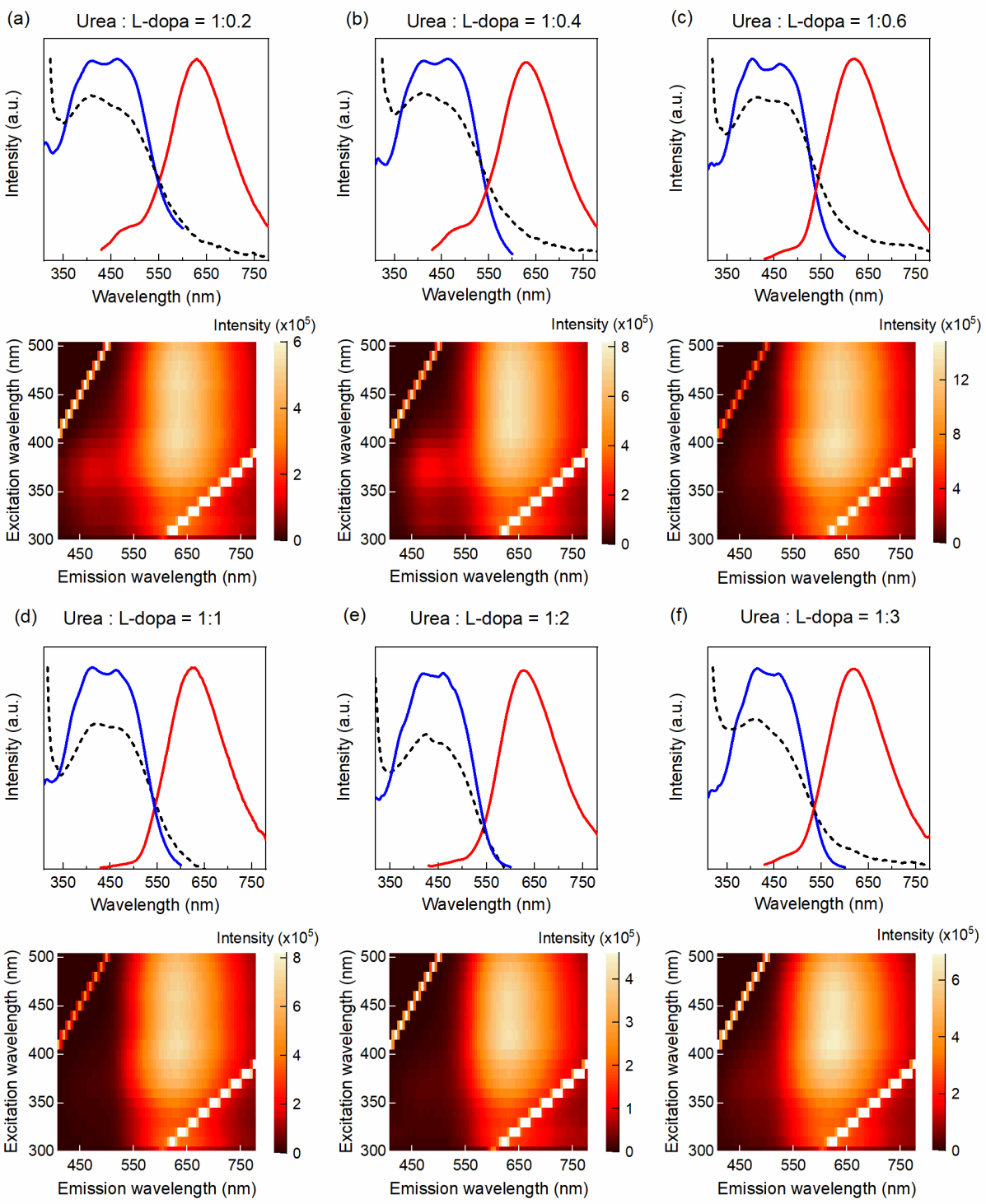

Figure S1. Absorption (black dashed), photoluminescence excitation (PLE) (blue solid), and photoluminescence (PL, solid red line) spectra, and PLE vs. PL density plots of R-CDs synthesized with various urea: L-dopa weight ratios of (a) 1:0.2, (b) 1:0.4, (c) 1:0.6, (d) 1:1, (e) 1:2, and (f) 1:3.

Table S1. Quantum yield (QY), PL peak maximum, and PLE peak maxima of R-CDs synthesized from different urea to L-dopa weight ratios.

Urea: L-dopa Ratio	1:0.2	1:0.4	1:0.6	1:1	1:2	1:3
QY [%]	13.4	17.0	31.0	45.2	14.7	14.9
PL [nm]	631	630	619	621	629	621
PLE [nm]	410, 463	410, 463	405, 462	407, 465	418, 460	414, 458

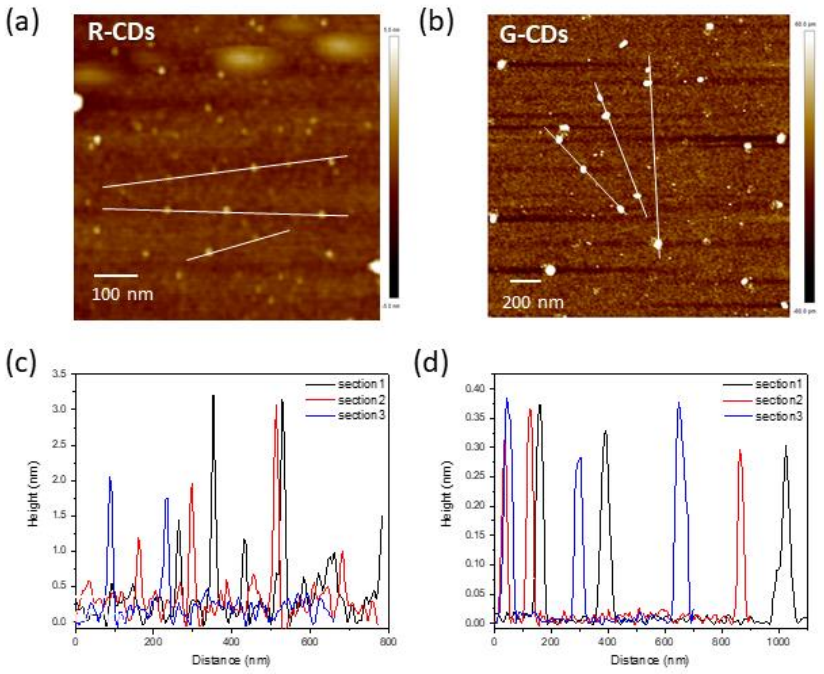

Figure S2. AFM images of (a) R-CDs and (b) G-CDs. The white lines are selected for height profiling. The 100 and 200 nm scale bars are shown in panels (a) and (b), respectively. (c) Height profiles of the three white lines selected in panel (a) of R-CDs. (d) Height profiles of the three white lines selected in panel (b) of G-CDs.

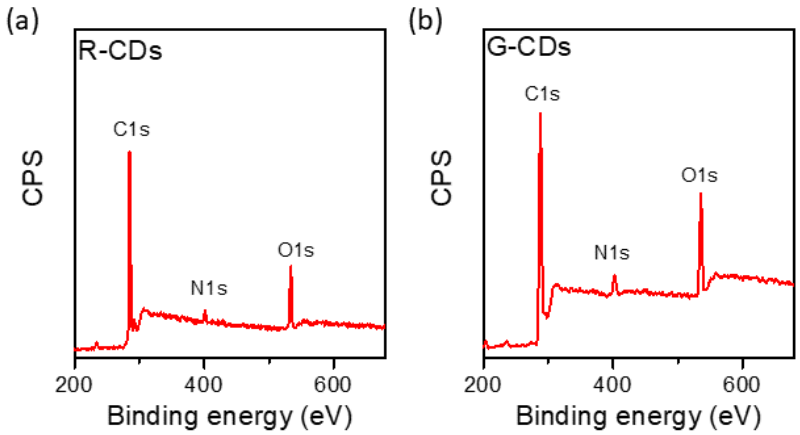

Figure S3. Full scan XPS spectra of (a) R-CDs and (b) G-CDs. Major peaks are denoted.

Table S2. C, N, and O content of R-CDs and G-CDs from XPS full spectra.

Element content	R-CDs	G-CDs
C	0.85	0.84
N	0.034	0.043
O	0.11	0.12

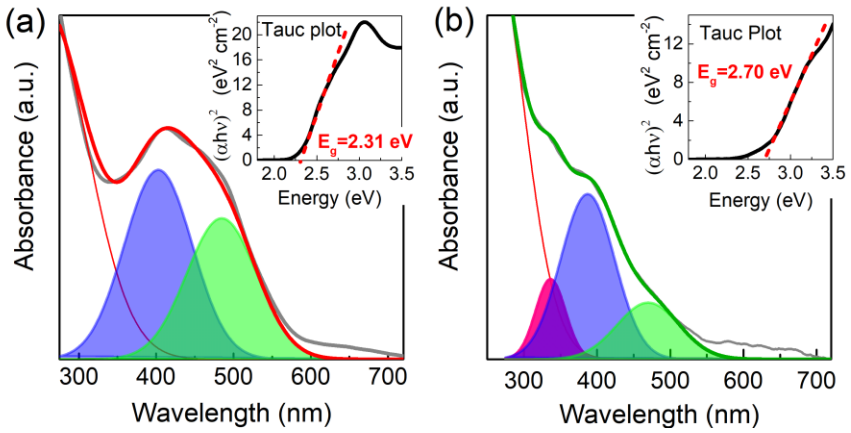

Figure S4. Steady-state electronic absorption spectra of (a) R-CDs and (b) G-CDs. Gaussian fitting was performed to extract the underlying absorption peaks: two peaks in panel (a) and three peaks in panel (b) are shown as semi-transparent color-coded peak shades, besides the large blue-absorbing peak below 300 nm (thin red curves). The best-fit absorption profiles are denoted by thick red and green lines for R-CDs and G-CDs in panels (a) and (b), respectively. The insets are the Tauc plots with the extracted optical bandgaps (E_g values).

Table S3. Stokes shift and emission wavelength summary for this work and previous reports of carbon dots with large Stokes shift

Reference	Excitation peak(nm)	Absorption peak(nm)	Emission peak(nm)	Stokes shift(nm)	QY (%)	Solvent
[1]	300	300	530	230	69.3	water
[2]	454	347	540	193	61	ethanol
[3]	374	233, 279	551	177	6.37	water
[4]	450	450	556	106	26	water
[5]	450	450	565	115	56	water
[6]	380	263, 387	568	188	24	water
[7]	450	267	570	120	31	water
[8]	440	275	590	150	15	DCM
[9]	510	492	603	111	41.1	n-amyl alcohol
[10]	550	270	650	100	42	formamide
[11]	521	288, 526	600, 661	79	41	DMSO
[12]	520	456	640	120	43, 36	ethanol, water
[13]	550	350,550	600	50	12.9	ethanol
This work (R-CDs)	270, 407	407	623	353	45.2	chloroform
This work (G-CDs)	270, 371	371	511	241	24.1	chloroform

DCM: dichloromethane

DMSO: dimethyl sulfoxide

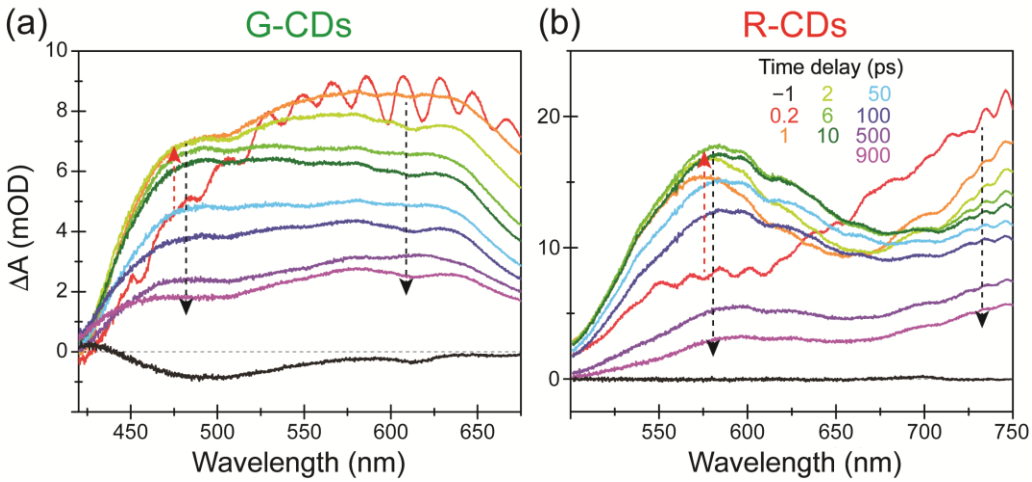

Figure S5. Time-stacked fs-TA spectra of (a) G-CDs and (b) R-CDs after 400 nm excitation. Red and black arrows denote the rise and decay of the ESA band intensity after the photoexcitation time zero, respectively, in the specific spectral regions that correspond to the probe-dependent plots in Figures 6c and 6d (main text). The mOD unit denotes milli-optical density in signal intensity. The selected time delay points across the detection time window are color-coded and shown in panel (b) inset.

References

1 Z.-H. Wen and X.-B. Yin, *RSC Adv.*, 2016, **6**, 27829–27835.

2 J. Li, H. Zhao, X. Zhao and X. Gong, *Nanoscale Horiz.*, 2023, **8**, 83–94.

3 Y. Xiao, W. Dong, H. Wang, Y. Hao, Z. Wang, S. Shuang, C. Dong and X. Gong, *Spectrochim. Acta A: Mol. Biomol. Spectrosc.*, 2021, **261**, 120028.

4 Q. Liu, X. Niu, K. Xie, Y. Yan, B. Ren, R. Liu, Y. Li and L. Li, *ACS Appl. Nano Mater.*, 2021, **4**, 190–197.

5 S. Zhang, H. Wang, Y. Li, F. Y. Data, Q. Wang and L. Jiao, *Mater. Lett.*, 2020, **263**, 127208.

6 F. Yan, Z. Bai, F. Zu, Y. Zhang, X. Sun, T. Ma and L. Chen, *Microchim. Acta*, 2019, **186**, 113.

7 S. Zhang, X. Ji, J. Liu, Q. Wang and L. Jin, *Spectrochim. Acta A: Mol. Biomol. Spectrosc.*, 2020, **227**, 117677.

8 V. Gude, A. Das, T. Chatterjee and P. K. Mandal, *Phys. Chem. Chem. Phys.*, 2016, **18**, 28274–28280.

9 T. Zhang, J. Zhu, Y. Zhai, H. Wang, X. Bai, B. Dong, H. Wang and H. Song, *Nanoscale*, 2017, **9**, 13042–13051.

10 M. Ali, A. S. Anjum, R. Riaz, A. Bibi, K. C. Sun and S. H. Jeong, *Carbon*, 2021, **181**, 155–168.

11 Y. Xian and K. Li, *Adv. Mater.*, 2022, **34**, 2201031.

12 H. Ding, J.-S. Wei, P. Zhang, Z.-Y. Zhou, Q.-Y. Gao and H.-M. Xiong, *Small*, 2018, **14**, 1800612.

13 X. Miao, D. Qu, D. Yang, B. Nie, Y. Zhao, H. Fan and Z. Sun, *Adv. Mater.*, 2018, **30**, 1704740.